Drug Development and Industrial Pharmacy, 34:373–383, 2008

ISSN: 0363-9045 print / 1520-5762 online
DOI: 10.1080/03639040701657792

informa
healthcare

A Novel Superdisintegrating Agent Made from Physically Modified Chitosan with Silicon Dioxide

Musa El-Barghouthi and Ala'a Eftaiha
Chemistry Department, Hashemite University, Zarqa, Jordan

Iyad Rashid, Mayyas Al-Remawi, and Adnan Badwan
Suwagh Company for Drug Delivery Systems Subsidiary of the Jordanian Pharmaceutical Manufacturing Co., Naor, Jordan

Disintegrants and fillers represent important excipients for immediate-release solid dosage forms in many pharmaceutical applications. A new excipient based on the coprecipitation of chitosan and silica has been achieved. The "intimate" physical association between chitosan and silica creates an insoluble, hydrophilic, highly absorbent material, consequently, resulting in superiority in water uptake, water saturation for gelling formation, and compactability among other superdisintegrants. The new excipient has an outstanding functionality that does not primarily depend on water wicking and swelling properties. In fact, it translates it into superior disintegration characteristics with improved powder flow and compaction properties. Thus, the new excipient could act as a superdisintegrant and pharmaceutical filler at the same time. Studies have shown that chitosan–silica delivers superior performance in wet granulation formulations and is the only disintegrant that is effective at all concentrations in tablet formulation.

Keywords superdisintegrant; chitosan–silica; coprecipitation

INTRODUCTION

A disintegrant is an excipient that is added to a tablet or capsule blend to aid in the break up of the compacted mass when placed in a fluid environment. This is especially important for immediate-release products, in which rapid release of drug substance is perquisite. A disintegrant can be added to a powder blend used for direct compression or encapsulation formulations. It can also be used with products that are wet granulated. In wet granulation formulations, the disintegrant is normally incorporated totally into the granule (intragranularly), or 50% (wt/wt) intragranularly and 50% (wt/wt) extragranularly, i.e., in the final dry mixture (Zhao & Augsburger, 2006).

Despite all theories proposed, however, there is still a lack of a full understanding of the mechanism of disintegration. Because all disintegrants are hygroscopic and draw liquid into the matrix, some investigators proposed a mechanism for the action of disintegrants based on water uptake through wicking, swelling, deformation (shape) recovery, particle repulsion, and heat of wetting (Augsburger, Brzecko, Shah, & Hahm, 2000). The swelling of disintegrant particles is perhaps the most widely accepted mechanism for tablet disintegration. Primarily, this is because almost all disintegrants swell to some extent (Gbenga & Oludele, 2003).

One of the most crucial factors in the disintegration process of many formulations is the water uptake caused by capillary forces. Khan and Rhodes (1975) studied the adsorption and absorption properties of various disintegrants. They concluded that the ability of particles to draw water into the porous network of a tablet is essential for efficient disintegration. As a general rule for most types of superdisintegrants, the higher the water uptake rate, the higher is the swelling capacity of the disintegrants (Caramella et al., 1989).

Classically, there are some tablet excipients such as starch and cellulose that are known to aid in disintegration. Starch has great affinity for water and swells when moistened, thus facilitating the rupture of the tablet matrix. This is due to its distinct capillary action, as the spherical shape of starch increases the porosity of tablet thus promoting capillary action (Lachman, Liberman, & Schwartz, 1989). Cellulose is reported to be effective as a disintegrant. It has a high swellability with water and ruptures the tablets into small particles (Tatsuya et al., 2001).

Recently, more effective agents are produced by chemical modification of starch, cellulose, and other polymers (such as povidone), and are referred to as superdisintegrants. They offer a more elegant formulation and reduction in size. The mechanism, by which their disintegration takes place, involves rapid absorption of water leading to an enormous increase in volume of granules, which results in rapid and uniform disintegration. The capillary and hydration activity of most superdisintegrants is mainly responsible for tablet disintegration property (Mukesh et al., 2007). Examples of the most widely used superdisintegrants

Address correspondence to Adnan Badwan, The Jordan Pharmaceutical Manufacturing Co. (PLC), IBN Sina Site, P.O. Box: 94, Naor 11710 Jordan. E-mail: suwagh@jpm.com.jo

are croscarmellose (cross-linked carboxymethyl cellulose), crospovidone (cross-linked polyvinyl pyrrolidone [PVP]), low-substituted hydroxypropyl cellulose (L-HPC), and sodium starch glycolate (Sakhr, Bose, & Menon, 1993). They are generally used at a low level in the solid dosage form, typically 1–10% by weight relative to the total weight of the dosage unit.

However, the currently available superdisintegrants are not ideal in their uses because of a number of limitations they practically impose on pharmaceutical applications. For example, the swelling of some disintegrant particles is dependent on the pH of the media (Shangraw, Mitrevej, & Shah, 1980). An acidic medium significantly reduces the liquid uptake rate and capacity of sodium starch glycolate and croscarmellose sodium, but not crospovidone (Chen, Lin, Cho, Yen, & Wu, 1997; Zhao & Augsburger, 2005).

In addition, Bussemer, Peppas, and Bodmeier (2003) described swelling as a time-dependent process with progressively increasing swelling energy and swelling force: croscarmellose had the highest degree of swelling under load, followed by L-HPC, whereas crospovidone and Methocel K100M® (hydroxypropyl methylcellulose) developed insufficient swelling.

Another important limitation to the use of swellable polymers in disintegration is justified by Zhao and Augsburger (2006) in wet granulation formulation. They illustrated that Primojel® (sodium starch glycolate) and Polyplasdone XL10® (crospovidone) exhibit a significant decrease in the rate of water being absorbed into the tablet matrix following wet granulation, but this was not observed for croscarmellose sodium. The increase in particle size following granulation appears to be the cause of the loss in disintegration efficiency.

In addition, medium ionic strength was found to have an adverse effect on the swelling capacity of superdisintegrants. The swelling of croscarmellose was found to be lower at higher ionic strength of the medium but was still significantly higher than the swelling of the other swellable superdisintegrants tested (Bussemer et al., 2003).

Therefore, in an attempt to overcome the shortcomings of these disintegrants, new approaches have been adopted recently in developing chemical and physical processes to modify natural biopolymers to serve as excipients in different pharmaceutical fields (Akbuga, 1995; Illum, 1998; Skaugrud, 1991). One of the latest and most interesting examples is chitin. It represents the second most abundant polysaccharide found in nature, next to cellulose. The main commercial sources of chitin are the shell wastes of shrimp, crab, lobster, krill, and squid. Chitin is mainly used for production of chitosan by a deacetylation reaction usually obtained in alkaline medium. Chitosan exhibits several favorable properties such as biodegradability and biocompatibility (Muzzarelli et al., 1998; Cerehira et al., 2003).

Chitosan has been developed for a variety of pharmaceutical applications, one of which has received a considerable attention in tablet disintegration applications (Giunchedi et al., 2002; Illum, Jabbal-Gill, Hinchcliffe, Fisher, & Davies, 2001; Lonso & Sanchez 2003). Tablets containing chitosan show faster disintegration and greater dissolution than those containing sodium starch glycolate and croscarmellose sodium. Moisture and water uptake were found to be the major mechanism of disintegration, whereas dissolution was related to swelling capacity of chitosan (Ritthidej, 1994).

However, when large-scale handling of pharmaceutical blends is desired, chitosan powder shows poor bulk density and therefore poor flowability and compressibility (Freyer & Brink, 2006). To overcome such weakness, chitosan has been recently modified by coprecipitation with colloidal silicon dioxide, which resulted in the improvement of chitosan's physical properties (Badwan & Al-Remawi, 2007). The choice of silicon dioxide was based on its unique high water absorption capacity and surface modification when being coprocessed with polymers. This was proven for microcrystalline cellulose and carboxymethyl cellulose (Soares, Ortega, Petrovick, & Schmidt, 2005; Van Veen & Bolhuis, 2005). Thus, colloidal silicon dioxide is an efficient candidate for the development and modification of highly compressible, highly compactable, and disintegrable excipients.

Therefore, there is a great need in this study to exploit the pharmaceutical and industrial potential of chitosan when being coprocessed with silica in terms of disintegration, dissolution, wet granulation, flowability, compression, and compaction over conventional superdisintegrants. Furthermore, the type of interaction between chitosan and silica is essential to be identified using infrared (IR) and X-ray analyses, and the mechanism of disintegration needs to be further investigated.

MATERIALS AND METHODS

Materials

The materials used were as follows: chitosan of pharmaceutical grade (Hong Ju Ginseng Co., Ltd., Dalian Liaoning, China, particle size < 150 μm, molecular weight 100,000 Da, 93% degree of deacetylation); colloidal silicon dioxide (Aerosil® 200, 120 nm, Evonik Degussa GmbH, Degussa, Germany); croscarmellose sodium (FMC Corp. Food and Pharmaceutical Division, Newark, DE, USA); sodium starch glycolate (Primojel®, Penwest Pharmaceuticals, Patterson, NY, USA); crospovidone (Kollidon® CL, BASF Aktiengesellschaft, Ludwigshafen, Germany); metformin HCl (Hercules Plaza, Wilington, NE, USA); Klucel EF® (Shouguang Huakang Pharmaceutical Trade Co., Shandong, China); and Talc® (Skyland Chemicals Corporation Ltd., Nanning Guangxi, China). All reagents used were of analytical grade.

Methods

In this research, two methods were adopted to formulate a superdisintegrant that had special physical properties. The two methods depended on the coprecipitation of silica particles onto chitosan particles by using either a dispersion of colloidal silica (chitosan–silica preparation) or a prepared aqueous sodium silicate solution (chitosan–silicate preparation). It should be

noted here that chitosan–silica and chitosan–silicate processes do not differ from each other in the concept of having insoluble silica particles precipitated on chitosan. Different terminologies, i.e., chitosan–silica and chitosan–silicate, are used in this study to differentiate between the two processes, although they both lead to the same final components of chitosan and silica. The details are described below.

Preparation of Chitosan–Silica

Five hundred grams of chitosan were dispersed in 1,000 mL of 2 M HCl. Approximately 500 g of colloidal silicon dioxide was dispersed in 1,000 mL of 2 M NaOH solution, to which 1,000 mL of deionized water was added under stirring until homogenization of the silica suspension was accomplished. The chitosan suspension was gradually added to the silica suspension at a rate of ~100 mL/min under vigorous stirring, which was continued for 1 h at ambient temperature (25°C) after completion of addition. The pH of the mixture was maintained not to exceed a pH value of 6.5, through mixing, by adjustment with concentrated HCl. The product was washed with deionized water until the conductivity of the filtrate, measured using a conductivity meter (Mettler Toledo MPC227, Mettler Toledo International, Inc., Greinfensee, Switzerland), was close to that of water. Then, the product was filtered out using 20–25 μm filter papers (Albet 135, Quantitative, Albet Filalbet, Barcelona, Spain). The filtrate was clear, as chitosan and/or silica particles cause turbidity when present. The product was dried in the oven at 90°C to complete dryness and finally passed over a mesh of 425 μm size. The product was stored in a well-sealed container for further testing the characterizations of the superdisintegrant.

Preparation of Chitosan–Silicate

This process was chosen because it would be practically easier to handle solutions (sodium silicate) instead of colloidal suspensions in the coprecipitation step). About 500 g of chitosan was suspended in 1,000 mL of 2 M HCl. Approximately 500 g of colloidal silicon dioxide was suspended in 1,000 mL of 2 M NaOH solution, to which 1,000 mL of deionized water was added under stirring until homogenization of the silica suspension was accomplished. The silica suspension was heated up to 80°C under stirring until a clear solution was obtained owing to the conversion of the insoluble suspended silicon dioxide into the soluble sodium silicate form. The chitosan suspension was gradually added to the silica suspension at a rate of ~100 mL/min under vigorous stirring, which was continued for 1 h at ambient temperature (25°C) after completion of addition. Concentrated HCl solution was added to lower the pH from 11 to 6.5. The product was washed, filtered, dried, and sieved as mentioned previously in the chitosan–silica preparation. However, the filtrate had a slight white turbidity, probably from micro-size particles (more likely silica; less than 20 μm) that had passed through the filter paper. Therefore, a silica mass balance was performed using inorganic content determination by ignition in the final product.

Inorganic Content Determination

Samples of chitosan, colloidal silicon dioxide, chitosan–silica, and chitosan–silicate were heated at 105°C for 3 h to remove the water content of the samples before ignition at 650°C using a furnace (Carbolite, Essex, UK), until constant weight was attained. The percentage of inorganic materials (residues), silicon dioxide in this case, was determined from the initial (after drying) and final weights (after ignition).

Scanning Electron Microscopy (FEI Quanta 200 3D SEM, FEI, Eindhoven, Netherlands)

Chitosan–silica and chitosan–silicate samples were mounted on aluminum stubs and then coated with gold by sputtering at 1,200 V, 20 mA, for 105 s using a vacuum coater.

X-ray Diffraction Powder Diffraction

The X-ray diffraction powder diffraction (XRPD) patterns of chitosan–silica, chitosan, and silica were measured using X-ray diffractometer (Philips PW 1729 X-Ray Generator, Philips, Eindhoven, Netherlands). X-ray powder diffraction runs were acquired on a Scintag Pad V X-ray Powder Diffractometer using Cu K_α radiation on a θ–2 θ goniometer equipped with a germanium solid-state detector. Acquisition conditions were 35 kV and 30 mA. Scans were obtained typically from 10 to 70° 2 θ, with step size or integration range of 0.05° 2 θ, with a count time of 5 s. Raw diffraction scans were stripped of kα2 (the continuous spectrum consisting of braking radiation and emission lines for electronic transitions caused by the metal anode material of the X-ray instrument) component, background-corrected with a digital filter (or Fourier filter), and peaks were identified using a variety of algorithms. Observed peak positions were matched against the ICDD JCPDS database on CDROM.

Fourier Transform Infrared Spectroscopy (Perkin-Elmer, Buckinghamshine, UK)

IR spectroscopy was used to determine the molecular interaction between chitosan and silica. For Fourier transform IR spectroscopy, chitosan–silica samples to be examined were mixed with dried KBr (1%, wt/wt). Then a small portion of the mixture was compressed in a special die at 1×10^5 kPa to yield a transparent disk. The disk was then held in the instrument beam for spectroscopic examination.

Bulk, Tap, and True Densities and Compressibility Index for Chitosan–Silica

For a chitosan–silica particle size of 190 μm, as measured by the Malvern Zeta-Sizer (3000HS, Malvern Instruments, Malvern, UK), the powder physical properties were specified. The bulk density was initially determined by pouring the powder (about 20 g) carefully into a glass cylinder; the density was then calculated by dividing the mass of the powder by the measured volume. For tap density, the cylinder was tapped for 10 min. The tap density was calculated in the same way as the bulk density,

as described above. Densities were determined as the mean of five measurements. The bulk and tapped densities of powders was compared to give an indication of the type of interaction present between the various particles making up the powder mass and hence provided an index of powder flowability as described by Taylor, Ginsburg, Hickey, and Gheyas (2000) The compressibility index was calculated according to the equation (Taylor et al., 2000)

$$\text{percent compressibility index} = 100 \times \frac{\text{tap density} - \text{bulk density}}{\text{tap density}} \quad (1)$$

The true density was determined (an average of five readings) using a helium pycnometer (Ultrapycnometer 1,000 v. 2.2, Quatachrome Co., Boynton Beach, FL, USA).

Angle of Repose

This technique is well illustrated in the United States Pharmacopoeia (USP30-NF25, 2007). Approximately 200 g of chitosan–silica powder was poured through a stainless-steel funnel from a height of 15 cm onto a level bench top. The angle that the side of the conical heap makes with the horizontal plane was recorded as the angle of repose. It was determined as the mean of five measurements. This technique has a direct indication of the potential flowability of a material. Lower angle of repose values represent better flow.

Tensile Strength vs. Relative Density

Powders from chitosan, chitosan–silica, chitosan–silicate, and the physical mixture (mass ratio of 1:1) of chitosan and silica (as Aerosil®) were compressed into 12-mm circular punch of a tablet weight of 400 mg at various pressure forces using a single-punch tableting machine (Manesty, Merseyside, UK). Relative density was calculated as the ratio of compact density to true density. Tablet hardness was measured using a hardness tester (Copley, Nottm Ltd, Therwil, Switzerland). From the measured tablet hardness, the tensile strength was calculated according to the equation (Leuenberger & Kuentz, 2000):

$$\sigma_t = \frac{2F}{\pi Dh} \quad (2)$$

where F is the tablet hardness, D the tablet diameter, and h the tablet thickness. The tensile strength vs. relative density correlations of the powders were compared.

Hygroscopicity

Different samples of chitosan–silica (initial weight of 2. g) were subjected to different humidity conditions of saturated salt solutions. The samples were placed in desiccators at ambient temperature (25°C). The media compositions were set according to the *Handbook of Chemistry and Physics*. The samples were stored in the desiccators for 1 week until equilibrium was reached. The percentage gain in weight from the original weight was measured for each humidity reading.

Maximum Water Saturation

To 25 mL of water, under stirring using magnetic stirrer, chitosan–silica powder was added stepwise, at room temperature, until the saturation end point was reached, indicated by the formation of solid mass of the powder and no further stirring required. The maximum saturation power of chitosan–silica was calculated by dividing the mass of the added powder by the fixed volume of water. This test was further performed on Primojel®, croscarmellose sodium and PVP-xl superdisintegrants. Each set of experiments was repeated five times, and the average was calculated.

Water Penetration Rate

Samples (0, 5, 20, and 50% [wt/wt]) were prepared by physically mixing chitosan–silica with microcrystalline cellulose (Avicel® 200, FMC Europe NV, Brussels, Belgium). The samples were poured individually into graduated cylinders to a fixed volume, 100 mL, without any applied pressure on the column of the resultant particles. To visualize and measure the water penetration into the samples, 50 mL of 0.1% (wt/vol) sunset yellow solutions was prepared and added to each of the prepared Avicel®–superdisintegrant samples. The penetration rate was calculated by measuring the speed of water (mL/min) penetrating the mixture columns. This method was validated on changing the dye concentration (0.11%), added volume of the dye solutions (10–100 mL), and the volume of the samples (50–200 mL). This test was further performed on Primojel®, croscarmellose sodium and PVP-xl superdisintegrants.

Disintegration Time

Disintegration time was measured using a disintegration tester (Caleva, Dorest, UK). Tablets examined were compressed into 13-mm circular punch of 470-mg weight at pressure forces of 30, 35, 40, and 50 kN using a single-punch tableting machine.

Heckle Plot Compressibility and Compactability Study of Chitosan–Silica

Chitosan–silica was compressed by direct compressing using the universal testing machine (UTM, RKM 50, PR-F system, ABS Instruments Pvt., Ltd., Leipzig, Germany). This was achieved without lubrication of the upper and lower punches as well as the die. Different compression forces from 25 to 390 MPa were applied. Three tablets were prepared to ensure reproducibility. The tablets were flat, round with 12 mm diameter, and of 400 mg weight. Compact porosity was calculated according to the equation (Leuenberger & Kuentz, 2000)

$$\varepsilon = 1 - \rho \quad (3)$$

where ε is the porosity and ρ the relative density.

Dissolution of a Model Drug Formula Containing Chitosan–Silica and Comparison with the Same Formula Containing Crospovidone

The functionality of chitosan–silica as a superdisintegrant was employed to drug formulas involving wet granulation processes. Metformin HCl was used as a model drug whereby the disintegration efficiencies of crospovidone and chitosan–silica, F1 and F2, respectively, were compared with each other when used extragranularly. The disintegration power, F3, of chitosan–silica was further examined when added intragranularly. A reference metformin HCl formula, F4, was prepared for comparison purposes with no disintegrants added.

The metformin HCl (with designed tablet strength of 500 mg) formula had the following components and percentages: metformin HCl 90.17%, Klucel EF® 3.69%, Klucel EF® (5% in alcohol) as the granulating agent 0.74%, purified Talc® 2.83%, and a superdisintegrant 2.57% (either crospovidone or chitosan–silica).

The dried powder was sieved using a 300-μm mesh prior to the addition of the disintegrant and lubricant. Finally, the formula was compressed using a 13-mm shallow concave punch at 35 kN. The tablet weight was fixed at 554 mg to contain 500 mg of the metformin HCl. Tablets were investigated according to hardness and disintegration time as well as dissolution. Dissolution was performed using 1,000 mL of phosphate buffer (pH 6.8) medium, USP apparatus I, at 50 rpm speed and 37°C.

Testing the Superdisintegration Power of Chitosan–Silica Among Commercial Superdisintegrants

About 100 g of a standard placebo mixture was prepared by mixing Avicel® 200 and lactose at a mass ratio of 70 and 30%, respectively. Then 20 g of mixture made from the standard placebo and a tested superdisintegrant was prepared before compaction using the single-press tableting machine at a pressure of 98 kN and using a 12-mm circular punch. The superdisintegrants tested were chitosan–silica, Primojel®, pregelatinized starch, PVP-xl, and croscarmellose sodium, all of which were added separately at different percentages (1, 5, 10, and 20%) to the standard placebo mixture. Tablet disintegration was performed for each mixture and for the placebo powder itself (compacted under the same conditions as the tested mixtures). Disintegration time was measured using a disintegration tester (Caleva, Dorest, UK).

RESULTS AND DISCUSSION

Silicon dioxide forms an insoluble colloidal suspension with water, whereas sodium silicate is a soluble, highly basic (pH 11.5) material that converts into insoluble silicon dioxide when the pH is lowered to 7.0 and below. When colloidal silicon dioxide is heated in concentrated NaOH solution, it converts into soluble sodium silicate solution (Maryyann & Pierre, 2003). These reactions were the starting point of chitosan–silica and chitosan–silicate processing.

Chitosan–silica processing was basically a precipitation of the partially negatively charged colloidal silica (suspended in 2 M NaOH) onto the positively charged chitosan (suspended in 2 M HCl). The pH of the final mixture was adjusted to neutrality causing agglomeration of chitosan that had silica particles adsorbed on its surface (Borzacchielo et al., 2001; Badwan & Al-Remawi, 2007). On the contrary, chitosan–silicate processing was a combination of two processes. The first process was a conversion of the soluble sodium silicate into colloidal particles of amorphous silica during the stepwise addition of the acidic chitosan suspension. This conversion usually takes place as the pH of sodium silicate solution is lowered (Maryyann & Pierre, 2003). The second was a precipitation of the partially negatively charged colloidal silica onto the positively charged chitosan. The pH of the final mixture was again adjusted to neutrality.

The two methods resulted in two coprecipitates with different characteristics. Tests were carried out to find which form was more suitable to be used in general formulations of pharmaceuticals.

The percentages of inorganic material calculated for chitosan, colloidal silicon dioxide, chitosan–silica, and chitosan–silicate were 0.1, 100, 50.2, and 35% (wt/wt), respectively, indicating complete precipitation of silicon dioxide in the case of chitosan–silica processing and 70% precipitation of silicon dioxide in the case of chitosan–silicate. This could explain the presence of white turbidity in the filtrate in the case of chitosan–silicate preparation, as small micro-size silica particles (< 20 μm) had passed through the filter papers.

The resultant powders were screened by scanning electron microscopy (SEM) and the difference in their appearances was clear, as shown in Figure 1. Chitosan (Figure 1A) had changed its native structure from thin, flat surface structure to three-dimensional compacts of chitosan–silica (Figure 1C) and chitosan–silicate (Figure 1D). Chitosan had no porous structure, whereas chitosan–silica had more porous structures compared with chitosan–silicate. Therefore, chitosan–silica has more exposed surfaces that, alternatively, would probably affect the physical properties of the powder (e.g., compactability).

Silica precipitation on chitosan particles has established partial crystalline characteristics of the physically amorphous chitosan. In fact, the term *noncrystalline* applies to materials that produce X-ray powder diffraction patterns composed of broad maxima. This was seen in the case of pure chitosan (Figure 2A) and pure silica (Figure 2). Pure chitosan showed a broad reflection at 24.8° and a relatively weak reflection centering at 14.9°, whereas pure silica showed no crystalline components. Upon coprecipitation, chitosan–silica powder showed some degree of crystallinity attributed first to the sharp narrow diffraction peaks at 45° and 53.5° and second to the slight decrease in pure chitosan amorphous peaks. Generally, the appearance of crystallinity could be attributed to chitosan that shows this increase either when the molecular weight is decreased or when it is being deprotonated (Dos Santos et al.,

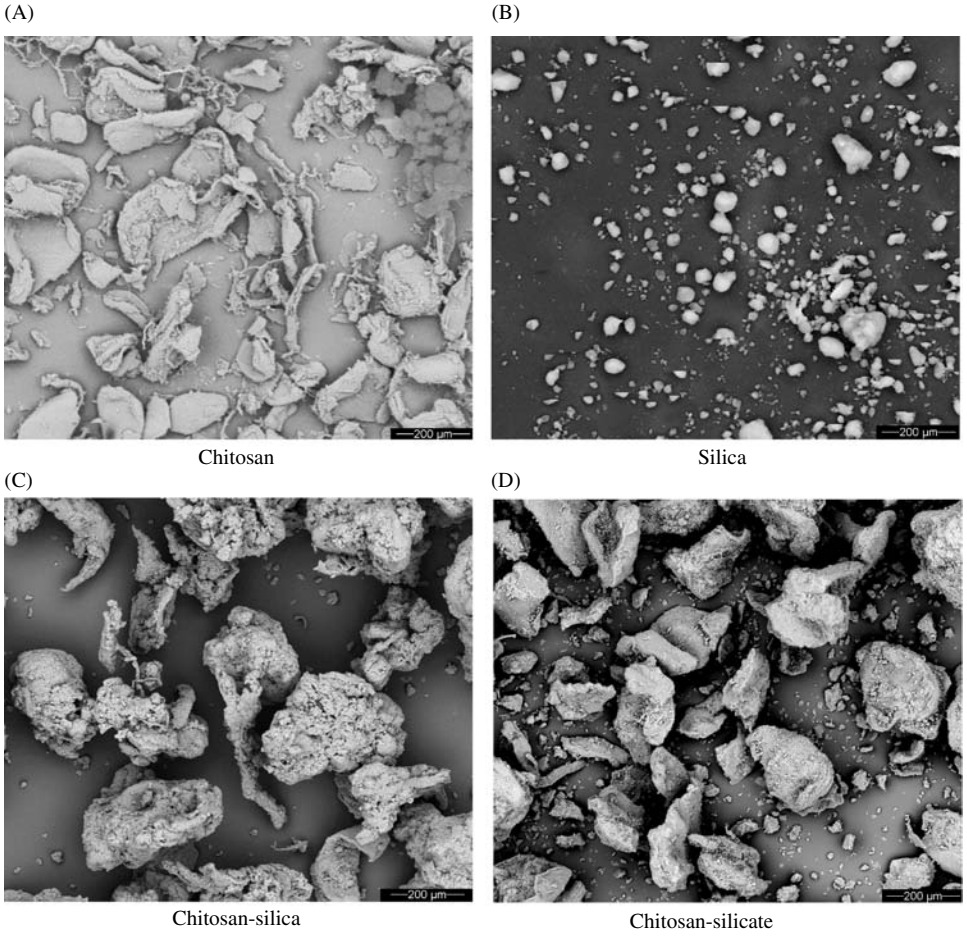

FIGURE 1. Scanning electron microscopic pictures of chitosan (A), silica (B), chitosan–silica coprecipitate (C), and chitosan–silicate coprecipitate (D).

2003; Nunthanid, Puttipipatkhachorn, Yamamoto, & Peck, 2001). The decrease in chitosan's molecular weight is possible to some extent through depolymerization in 2 M HCl, as no heating was induced. Deprotonation is more likely to cause such crystallinity, as chitosan was converted from the protonated form (chitosan.HCl) in 2 M HCl into chitosan when the pH of the chitosan–silica mixture was adjusted to neutrality. However, this did not exclude the amorphous characteristics of the chitosan–silica, which were still presented by the broad reflection at chitosan–silica complex.

The appearance of crystalline characteristics on coprecipitation was further illustrated using Fourier transform (FT) IR analysis of the pure components and the coprecipitate (see Figure 3). Pure chitosan showed a distinct C = O and NH_2 bands at 1,650 and 1,580 cm^{-1}, respectively (Cerai, Guerra, & Tricoli, 1996). These bands were noticed to become sharper in shape on coprecipitation of silica on chitosan, indicating the formation of crystalline compounds. In addition, the FTIR spectrum of chitosan, silica, and chitosan–silica coprecipitate did not represent a chemical reaction type. This could be supported by the fact that there was no reduction of the main amide peak at 1,580 cm^{-1} (Figure 3), as this band is normally known to be highly interactive. Therefore, the FTIR of chitosan–silica coprecipitate was almost similar to that obtained by physically mixing the two components as illustrated in Figure 3. Hence, the preparation method did not involve any chemical reaction, and just a physical modification occurred on the particles' surfaces.

This close association between chitosan and silica or silicate without evidence of covalent bonding (as indicated by the FTIR analysis) and ionic interactions (as coprecipitation was brought to neutrality) suggests that silica or silicate ions interact with the glucopyranose rings of chitosan, presumably through dipole–dipole and hydrogen-bonding interactions.

Theoretically, crystalline characteristics of powders, in general, yield compacts of less tensile strength and subsequently shorter disintegration time (Kothari, Kumar, & Banker, 2002). However, the tensile strength of chitosan–silica or chitosan–silicate was found higher than that obtained for chitosan alone as seen in Figure 4. Thus, the hard compacts of chitosan–silica obtained oppose the crystallinity–tensile strength relationship. Chitosan–silica, as seen in Figure 2C, maintained a great deal of amorphous characteristics, reflected by the broad band at

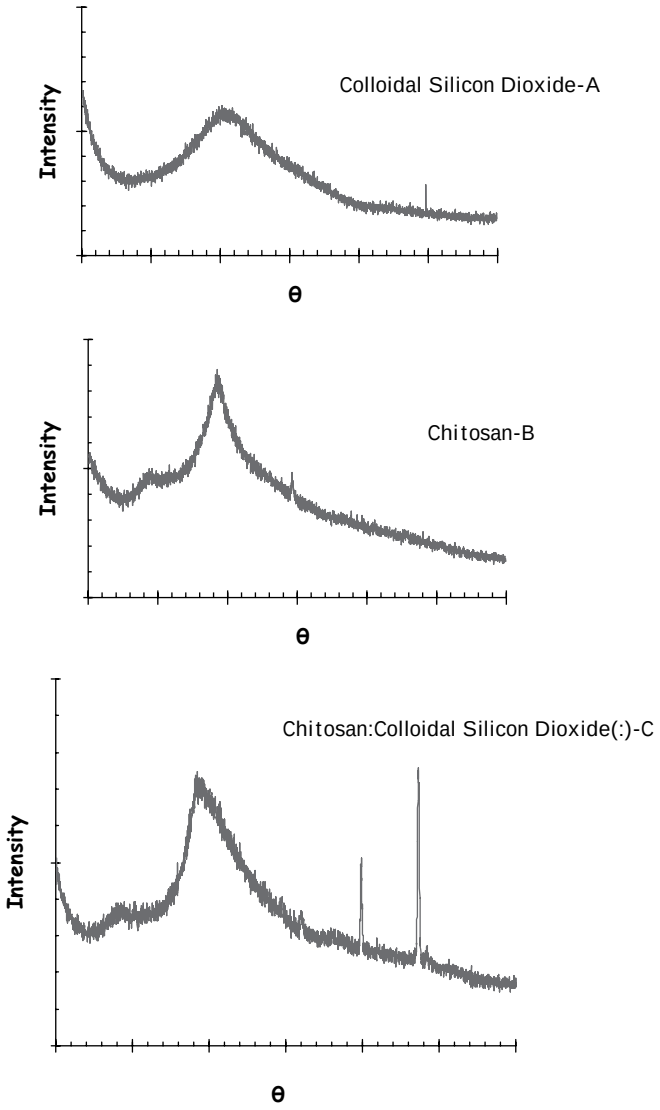

FIGURE 2. X-ray diffraction of silica (A), chitosan (B), and the coprecipitate (C).

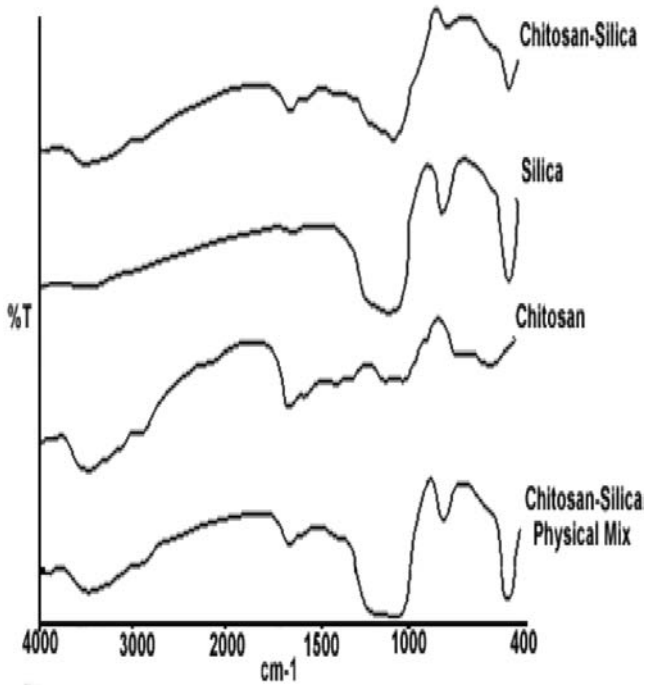

FIGURE 3. IR spectra of chitosan, silica, their physical mix, and their coprecipitate.

24.8°. The presence of this band could contribute to the high compactability of the new superdisintegrant, as would be explained in the discussion.

One of the important characteristics investigated for chitosan–silica as a superdisintegrant was hygroscopicity. Disintegration power is dependent on water uptake, and alternatively, on powder hygroscopicity. Polymers with a higher moisture uptake capacity will be expected to be more prone to impairment of tablet disintegration time. The hygroscopicity measured for chitosan–silica, as shown in Figure 5, clearly indicated that chitosan–silica was capable of gaining moisture up to 30% of its initial weight. In general, the moisture adsorptive capacity of chitosan–silica increases as the relative humidity is increased. However, hygroscopicity was not highly significant when chitosan–silica was subjected to humidity conditions below 70%. Such property may be taken as an advantage, where environmental conditions as anticipated are not a real threat to integrity of such product. The same pattern was observed for the hygroscopicity of fumed silica particles (Robert & Vojko, 2005). Thus, chitosan–silica moisture adsorptivity would be mainly attributed to silica particles associated with chitosan or to the presence of the large number of hydroxyl sites on the surface. Silicon dioxide hygroscopicity is a result of an interaction with water due to the locally strained bonds, with reduced bond energy of silicon dioxide at the molecular level,

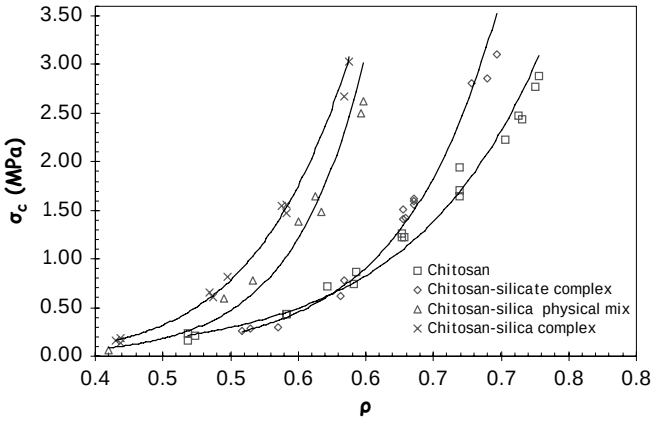

FIGURE 4. Tensile strength vs. relative density of chitosan, chitosan–silica physical mix, and chitosan–silicate and chitosan–silica complexes.

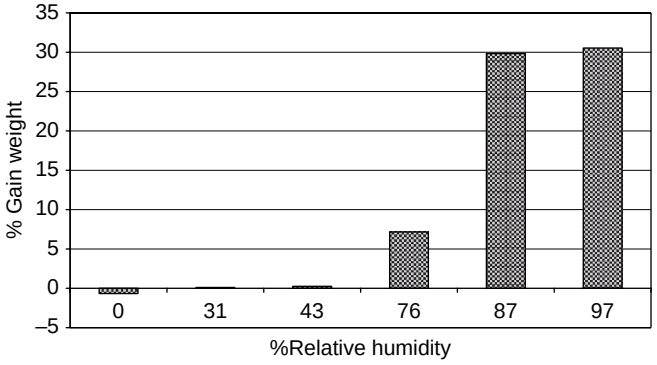

FIGURE 5. Hygroscopicity test for chitosan–silica performed using standard salt solutions of different humidity conditions stored inside desiccators at room temperature for 1 week.

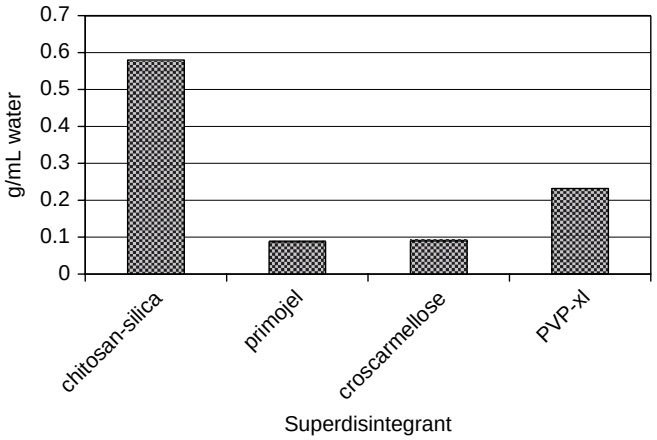

FIGURE 6. Maximum amounts of various superdisintegrants needed to form a gel layer upon gradual addition to water.

which makes it particularly vulnerable to attack by water, i.e., hydrolysis (Vansant, Van Der Veport, & Vrancken, 1995).

The degree of interaction between silica and chitosan in the complex was tested in 0.1 M HCl medium. Basically, when the complex was added to a volume of 0.1 M HCl with vigorous stirring in the form of powder or tablets, a viscous white suspension appeared. The increase in viscosity was a result of chitosan being dissolved in the dilute acidic medium, and the white turbidity was a result of suspended silica particles. Theoretically, these are the solubility properties of chitosan and silica in dilute acids (*Handbook of Chemistry and Physics*, 1975; Pankaj & Lawrence, 1999). This may indicate that the interaction between chitosan and acidic medium is greater than that between chitosan and silica.

Such interaction has to be considered to understand the mechanistic action of chitosan–silica on disintegration. Therefore, two distinct characteristics were investigated and compared with other commercial superdisintegrants: maximum water saturation and water penetration rate.

As the concentration of all commercial superdisintegrants increases within the tablets, the swelling rate becomes so high that they form a gel-like layer that blocks the passage of water inside deeper layers. The formation of the gel layer is a result of an increase in the viscosity of the medium surrounding the particles due to hydration of the particles (Marina & Ali, 2004). This makes common superdisintegrant play their role on the interface. Therefore, it was essential to examine the maximum amount of the superdisintegrants added to a fixed volume of water needed to form the gel layer. Figure 6 indicates that water can accommodate larger masses of chitosan–silica before gelling occurs than is the case for the other commercial superdisintegrants.

Water penetration rate of chitosan–silica column and other superdisintegrants was determined to further highlight the mechanistic action of superdisintegrants; this is shown in Figure 7. The choice of using Avicel® mixed with tested superdisintegrants was based on its free allowance to water passage without any hindrance due to gelling. It was clear that water could penetrate Primojel® and croscarmellose sodium only when their percentages were within their limits of use, as described in the *Handbook of Excipients*, and at the same rate as that of Avicel® 200. This means that their presence within the limits cannot hinder the passage of water. It is only when their concentrations are increased above their limits (i.e., > 10%), water can no longer pass through due to the swelling action of Primojel® and croscarmellose sodium. PVP-xl showed good water penetration rate, nearly up to double the rate shown by Avicel® alone. However, this was only encountered when the PVP-xl concentration was 5–10%; at higher concentrations, there would be a decrease in the rate due to obstruction by the PVP-xl. Chitosan–silica showed the highest water penetration rate without limits to its content within the Avicel®–superdisintegrant mixture.

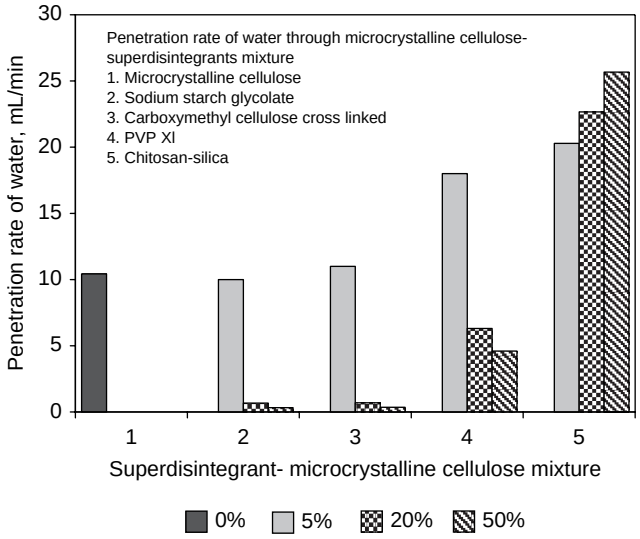

FIGURE 7. Water penetration rates of chitosan–silica and other commercial superdisintegrants (Primojel®, croscarmellose, and crospovidone) mixed with Avicel® at the superdisintegrants' concentrations of 0, 5, 20, and 50%.

Therefore, the action of chitosan–silica would be independent of its concentration within solid dosage forms.

The powder compressibility index was calculated from the measured bulk density 0.38 g/mL and tap density 0.41 g/mL, according to Equation 1. Thus, the resulting powder compressibility index value of 7.3% would categorize this type of powder as an excellent flowable material according to the United States Pharmacopoeia (USP30-NF25, 2007). This was further confirmed by the angle of repose measured at an average value of 28° for chitosan–silica powder. At this value, the powder flowability is categorized as excellent (USP30-NF25, 2007). When this flowable, good compressible material was compressed into tablets at different compression forces, the superdisintegration power was noticed to be independent of tablets' hardness, as shown in Table 1. Thus, the actions of water uptake and capillary penetration were more dominant than the counteraction caused by tablet hardness.

The Heckel's plots (Figure 8 for the high-molecular-weight chitosan and the chitosan–silica powders showed no linearity at early stages of compression because of particle rearrangement and the fragmentation of large aggregates under low compression pressures (Ilkka & Paronen, 1993). When the compression force is increased, the curves become linear because of plastic deformation. The slope of the Heckel's plot

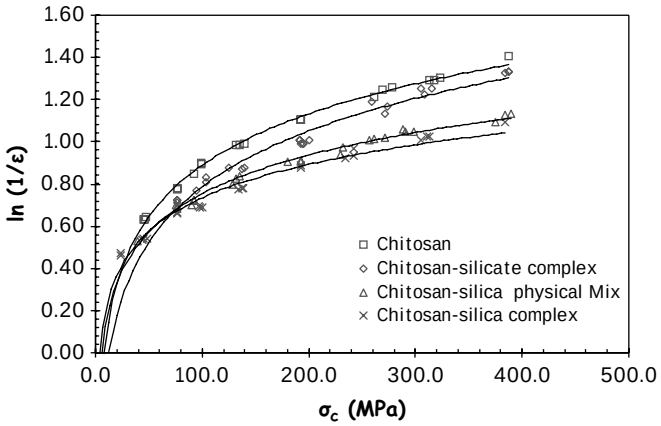

FIGURE 8. Heckel's plots of chitosan, chitosan–silica physical mix, and chitosan–silicate and chitosan–silica complexes.

(k) is indicative of the plastic behavior of the material (Paronen & Iilla, 1996). A higher value for the slope is related to a larger amount of plasticity in the material. Both chitosan and chitosan–silica had the same slope, and because chitosan is evaluated as directly compressible material (Knapczyk, 1993), the new superdisintegrant's compressibility and compactability would, therefore, be as high as that achieved using chitosan.

Thus, the surface modification of chitosan by silica or silicate resulted in a shift toward a compactable form, which is generally attributed to the decrease in the compacts' pore size, compared with chitosan, as could be deduced from the Heckle's plot. In addition, there might be some contribution of such pore size effect on chitosan–silica's superdisintegration capacity. When tablets are compacted to higher hardness values, disintegration time takes longer (almost linearly on a log scale) as the pores become smaller in size (Rawas-Qalaji, Simons, & Simons, 2006).

The product's integrity was tested over wet granulation formulations. It was found that wet granulation did not alter the functionality of chitosan–silica as a superdisintegrant, as intrangranular (F3) and extrangranular (F2) additions achieved the same release behavior of metformin HCl, as shown in Table 2. A full release of the drug was obtained within 5 min of

TABLE 1
Disintegration Time of Chitosan–Silica Tablets at Different Compression Forces

Force (kN)	Hardness (N)	Disintegration Time (s)
30	55	< 5
35	60	< 5
40	65	< 5
50	95	< 10
98	123	< 10

Tablets examined were compressed into 13-mm circular punch of 470 mg weight.

TABLE 2
Comparison of Chitosan–Silica Added Extragranularly and Intragranularly with Crospovidone in Metformin HCl Formulas, Which Were Compressed Using a 13-mm Shallow Concave Punch at 35 kN

Formula	Disintegrant	Addition Condition	Hardness (N)	Disintegration Time (min)	5 min Dissolution (%)	10 min Dissolution (%)
F1	Crospovidone	Extragranular	72	1.0	87.7	99.2
F2	Chitosan–silica	Extragranular	77	< 1.0	100	100
F3	Chitosan–silica	Intragranular	76	< 1.0	100	100
F4	No disintegrant	—	75	8.0	—	—

The dissolution was performed according to the USP test in terms of the medium, but apparatus I was used and the speed was 50 rpm.

TABLE 3
Testing the Superdisintegration Power of Chitosan–Silica Among Commercial Superdisintegrants

	Disintegration Time at Different Disintegrants Percentages				
Material	1	5	10	20	100
Primojel®	< 50 s	< 30 s	< 30 s	< 50 s	> 10 min
Pregelatinized starch	< 1.0 min	< 30 s	< 30 s	< 20 s	> 5 min
PVP-xl	< 50 s	< 40 s	< 30 s	< 20 s	> 10 min
Croscarmellose Na	< 50 s	< 30 s	< 30 s	< 30 s	> 10 min
Chitosan–silica	< 50 s	< 20 s	< 10 s	< 10 s	< 5 s
Placebo as blank			> 10.0 min		

Tablets weight was fixed at 500 mg. The tablets were compressed at a pressure of 1 ton and using a circular punch of 12 mm diameter.

the dissolution time at 2% of chitosan–silica. The impact of disintegration of chitosan–silica on dissolution was even higher than that for crospovidone when added extragranularly (F1), as a full drug release was only achieved in 10 min of dissolution time.

Finally, the superdisintegration competence of the naturally fibrous silicated form of chitosan was set in parallel with selected commercial ones (see Table 3). The low concentration of chitosan–silica in tablets was as efficient as Primojel® and croscarmellose and better than crospovidone. The most interesting feature could be seen when disintegration time became elevated when the concentrations of the commercial superdisintegrants were increased above their limits. This result could be explained from the data obtained previously from the maximum water saturation and water capillary penetration, as shown in Figures 5 and 6. Chitosan–silica, as seenin Table 3 was the only unique and distinctive superdisintegrant that maintained its functionality at all concentration ranges within the tablet dosage forms.

CONCLUSIONS

In summary, chitosan–silica has demonstrated improved disintegration and dissolution functionality over conventional superdisintegrants. SEM revealed that silicon dioxide, in some manner, has been integrated with chitosan particles via a partial coating of the particles, without any chemical interaction of the two ingredients as evidenced by IR analysis. This association has been confirmed by X-ray diffraction whereby the amorphous chitosan particles gained some crystalline characteristics. Heckel's plot analysis revealed that the superdisintegrant plastically deforms under applied pressure, which allows it to be used in direct compression applications. Moreover, the high hygroscopicity and high water capillary penetration turn to be the driving engine for such superdisintegration. Finally, the improved flow and the ability to be implemented in wet and dry granulation with no concentration limits of the superdisintegrant can impart further benefit in pharmaceutical applications.

REFERENCES

Akbuga, J. (1995). A biopolymer: Chitosan. *Int. J. Pharm. Adv., 1*, 1–18.

Augsburger, L. L., Brzecko, A. W., Shah, U., & Hahm, H. A. (2000). Characterization and functionality of super disintegrants. In J. Swarbrick & J. C. Boylan (Eds.), *Encyclopedia of pharmaceutical technology* (pp. 269–291). New York: Marcel Dekker.

Badwan, A., & Al-Remawi, M. (2007). Chitosan-silicon dioxide coprecipitate as an excipient in solid dosage forms. *Eur. Pat. Appl.,* 23. Jordan: The Jordanian Pharmaceutical Manufacturing Co.

Borzacchielo, A., Ambrosias, L., Netter, P., Nicholais, L., Balard, A., & Sam, P. (2001). Chitosan-based hydrogels: Synthesis and characterization. *J. Mater. Sci.: Mater. Med., 12*, 861–864.

Bussemer, T., Peppas, N. A., & Bodmeier, R. (2003). Evaluation of the swelling, hydration and rupturing properties of the swelling layer of a rupturable pulsatile drug delivery system. *Eur. J. Pharm. Biopharm., 56*, 261–270.

Caramella, C., Ferrari, M., Ronchi, A., Gazzaniga, U., Conte, A. L., & La Manna, A. (1989). Relationships between water uptake and disintegration force in tablets of differing solubility. *Congres. Int. Technol. Pharm., 3*, 256–265.

Cerai, P., Guerra, G. D., & Tricoli, M. (1996). Polyelectric complexes obtained by radical polymerization in the presence of chitosan macromolecular chemistry and physics. *Macromol. Chem., 197*, 3367.

Cerehiara, T., Luppi, B., Bigueei, F., & Zeeehi, V. (2003). Chitosan and salts as nasal sustained delivery systems for peptidic drugs. *J. Pharm. Pharmacol., 55*, 1623–1627.

Chen, C. R., Lin, Y. H., Cho, S. L., Yen, S. Y., & Wu, H. L. (1997). Investigation of the dissolution difference between acidic and neutral media of acetaminophen tablets containing a super disintegrant and a soluble excipient. *Chem. Pharm. Bull., 45*, 509–512.

Dos Santos, D. S., Bassi, A., Rodrigues, J. J., Miosoguti, L., Oliveira, O. N., & Mendonac, C. R. (2003). Light-induced storage in layer-by-layer films of chitosan and an azo dye. *Biomacromolecules, 4*(6), 1502–1505.

Freyer, K. M. P., & Brink, D. (2006). Evaluation of powder and tableting properties of chitosan. *AAPS PharmSciTech., 7*(3), Article 75.

Gbenga, A., & Oludele, A. I. (2003). Effects of starches on the mechanical properties of paracetamol tablet formulations. II. Sorghum and plantain starches as disintegrants. *Acta. Pharm., 53*, 313–320.

Giunchedi, P., Juliano, C., Gavini, E., Cossu, M., & Sorrenti, M. (2002). Formulation and in vivo evaluation of chlorhexidine buccal tablets prepared using drug-loaded chitosan microspheres. *Eur. J. Pharm. Biopharm., 53*, 233–239.

Ilkka, J., & Paronen, P. (1993). Prediction of the compression behavior of powder mixtures by the Heckel equation. *Int. J. Pharm., 94*, 181–187.

Illum, L. (1998). Chitosan and its use as a pharmaceutical excipient. *Pharm. Res., 15*, 1326–1331.

Illum, L., Jabbal-Gill, I., Hinchcliffe, M., Fisher, A. N., & Davis, S. S. (2001). Chitosan as a novel nasal delivery system for vaccines. *Adv. Drug. Deli. Rev., 51*(81), 1–3.

Khan, K. A., & Rhodes, C. T. (1975). Water-sorption properties of tablet disintegrants. *Pharm. Sci., 64*(3), 447–451.

Knapczyk, J. (1993). Excipient ability of chitosan for direct tableting. *Int. J. Pharm., 89*, 1–7.

Kothari, S. H., Kumar, V., & Banker, G. S. (2002). Comparative evaluations of powder and mechanical properties of low crystallinity celluloses, microcrystalline celluloses, and powdered celluloses. *Int. J. Pharm., 232*(1–2), 69–80.

Lachman, L., Liberman, L., & Schwartz, J. (1989). *Pharmaceutical dosage forms, tablets* (Vol. 2; pp. 173–177). New York: Marcel Dekker.

Leuenberger, H., & Kuentz, M. (2000). A new theoretical approach to tablet strength of a binary mixture consisting of a well and a poorly compactable substance. *Eur. J. Pharm. Biopharm., 49*, 151–159.

Lonso, M. J., & Sanchez, A. (2003). The potential of chitosan in ocular drug delivery. *J. Pharm. Pharmacol., 55*, 1451–1463.

Marina, L., & Ali, R. R. S. (2004). The influence of excipients on drug release from hydroxypropyl methylcellulose matrices. *J. Pharm. Sci., 93*(11), 2746–2753.

Maryyann, F., & Pierre, D. (2003). Research universities and local economic development: Lessons from the history of Johns Hopkins University. *Industry Innovation, 10*(1), 5–24.

Mukesh, C, G., Rajesh, K. P., Bansari, K. B., & Aarohi, R. S. (2007). Preparation and assessment of novel coprocessed superdisintegrant consisting of crospovidone and sodium starch glycolate. *AAPS PharmSciTech., 8*(1), Article 9.

Muzzarelli, R. A. A., Baldassare, V., Conti, F., Gazzanelli, G., Vasi, V., Ferrara, P., & Biangini, G. (1988). The biological activity of chitosan: Ultrastructural study. *Biomaterial, 8*, 247–252.

Nunthanid, J., Puttipipatkhachorn, S., Yamamoto, K., & Peck, G. E. (2001). Physical properties and molecular behavior of chitosan films. *Drug Dev. Ind. Pharm., 27*, 143–157.

Pankaj, R. R., & Lawrence, H. B. (1999). Chitosan processing: Influence of process parameters during acidic and alkaline hydrolysis and effect of the processing sequence on the resultant chitosan's properties. *Carbohydr. Res., 321*, 235–245.

Paronen, P., & Iilla, J. (1996). Porosity-pressure functions. In, G. Alderborn & C. Nystrom (Eds.), *Pharmaceutical powder compaction technology* (pp. 55–75). New York: Marcel Dekker.

Rawas-Qalaji, M. M., Simons, F. E. R., & Simons, K. J. (2006). Fast-disintegrating Sublingual Tablets: Effect of Epinephrine load on tablet characteristics *AAPS PharmSciTech., 7*(2) Article 41.

Ritthidej, G. C., Chomoto, P., & Pammangusa, S. (1994). Chitin and chitosan as disintegrants in paracetamol tablets. *Drug Dev. Ind. Pharm., 20*(13), 2109–2114.

Robert, R., & Vojko, K. (2005). Evaluation of the moisture sorption behaviour of several excipients by BET, GAB and microcalorimetric approaches. *Chem. Pharm. Bull., 53*(6), 662–665.

Sakhr, A., Bose, M., & Menon, A. (1993). Comparative effectiveness of super disintegrants on the characteristics of directly compressed triamterene hydrochlorothiazide tablets. *Pharm. Ind., 55*, 953–957.

Shangraw, R. F., Mitrevej, A., & Shah, M. (1980). A new era of tablet disintegrants. *Pharm. Technol., 4*(10), 49–57.

Skaugrud, O. (1991). Chitosan-new biopolymer for cosmetics and drugs. *Drug Cosmetic Ind., 148*, 24–29.

Soares, L. L., Ortega, G. G., Petrovick, P. R., & Schmidt, P. C. (2005). Optimization of tablets containing a high dose of spray-dried plant extract: A technical note. *AAPS PharmSciTech., 06*(03), E367–E371.

Tatsuya, I., Baku, M., Shuji, S., Naoki, U., Makiko, F., Mitsuo, M., & Yoshiteru, W. (2001). Preparation of rapidly disintegrating tablets using new type of MCC (PH-M-series) and L-HPC by direct compression method. *Chem. Pharm. Bull., 49*(2), 134–139.

Taylor, M. K., Ginsburg, J., Hickey, A., & Gheyas, F. (2000). Composite method to quantify powder flow as a screening method in early tablet or capsule formulation development. *AAPS PharmSciTech., 1*(3), Article 18.

Van Veen, B., & Bolhuis, G. K. (2005). Compaction mechanism and tablet strength of unlubricated and lubricated (silicified) microcrystalline cellulose. *Eur. J. Pharm. Biopharm., 59*(1), 133–138.

Vansant, E. F., Van Der Veport, P., & Vrancken, K. C. (1995). *Characterization and chemical modification of silica surface* (chap. 8.3). Amsterdam, New York: Elsevier Science Publishing.

Weast, R.C. (Ed.). (1974–1975). *Handbook of chemistry and physics* (55th ed.; p. E-46). Boca Raton, FL: CRC Press.

Zhao, N., & Augsburger, L. L. (2005). The influence of swelling capacity of super disintegrants in different pH media on the dissolution of hydrochlorothiazide from directly compressed tablets. *AAPS PharmSciTech., 6*(01), 120–126.

Zhao, N., & Augsburger, L. L. (2006). The influence of granulation on super disintegrant performance. *Pharm. Dev. Technol., 11*(1), 47–53.

United States pharmacopeia and national formulary (USP30-NF25: Vol. 1, p. 644). (2007). Rockville, MD: US Pharmacopoeia Convention.